VI International Conference on Computational Methods for Coupled Problems in Science and Engineering
COUPLED PROBLEMS 2015
B. Schrefler, E. Oñate and M. Papadrakakis (Eds)

# FLUID-THERMAL-STRUCTURE COUPLED ANALYSIS OF GRID FINS FOR HYPERSONIC FLIGHT VEHICLE

**SHENGZE LI*, ZHENYU JIANG*, WEIHUA ZHANG* AND KE PENG***

* College of Aerospace Science and Engineering
National University of Defense Technology
109 Deya Road, 410073 Changsha, China
e-mail:lsz86591989@163.com

**Key words:** Grid Fin, Hypersonic, Fluid-Thermal-Structure Coupling, Angle of Attack, Thermal Protection.

**Abstract.** The aim of this work is to provide a numerical method of fluid-thermal-structure coupled simulation of grid fins in hypersonic flows. Hypersonic flight vehicle with grid fins offers many advantages under high speed condition. The main advantages are small hinge moments, efficient packaging and capability to produce effective aerodynamic force at high angles of attack over wide Mach number ranges. The structure, however, sustains complicated loads caused by aerodynamic forces and heating during hypersonic flight. The large aggregations of experimental studies are limited to parts of physical characteristic due to the difficulty in the data transmission. This study takes the full influence of fluid flow into account as well as heat transfer on structure strength and stiffness. The following work is done. Firstly, Reynolds-Averaged approach and Spalart-Allmaras turbulence model are employed to solve the problem of flowing fluid. The simulation is achieved by using second order upwind scheme and hexahedral mesh grids. Validation has done by comparing the computed normal force coefficient with wind tunnel data for a Mach number from 1.8 to 3.5 and different angles of attack. Secondly, computations are performed at free stream Mach number 6 at five angles of attack from 0 to 15 degrees. The data of aerodynamic forces and heat flux is obtained after fluid-thermal coupled calculation. The strength and stiffness calculations are carried out by taking the aerodynamic forces and heat flux as boundary condition of solid domain. Finally, two types of structure form are discussed for long time thermal protection. One is niobium alloy, the other is C/SiC composites. The article shows that different thermal and mechanical predictions are affected by various conditions such as angle of attack, material characteristics. The structure response takes on a whole different status under different angles of attack. This allows engineers to choose appropriate size and type for hypersonic thermal protection materials.

## 1 INTRODUCTION

With the comprehensive and integrated development of engineering system, researches on some problems are no longer confined to a single discipline, and the multi-physics coupling analysis is a universal example. The analysis often requires different processes simulations for the same region in order to get some results of two or more field interactions. Therefore, it's a

great challenge for the research of multi-field couplings and its application in engineering problems, and the coupling mechanism has become a research focus of many disciplines.

Grid fin is a nonconventional aerodynamic lifting and control surface consisting of an outer frame with internal lattice[1]. In the 1940s, scientists from the Soviet Union first carried out theoretical and experimental researches of the grid fin[2, 3] in aerodynamics, structure, strength, quality, and manufacturing process, but because of lack of knowledge of various features of such wing surface, the grid fin was not widely used. In recent years, the grid fin has again attracted the attention of the world. Russia, United States, Germany and China have strengthened theoretical researches and experimental development of grid fin and have successfully applied it to satellites, rockets and missiles. After that, many advantages of grid fin have been proved by the studies such as low hinge moment, efficient packaging, suitability of tube launching and good lifting characteristics in supersonic or hypersonic flows[4-7]. Naturally, with the hypersonic techniques development, the researches of grid fin are also extended to the field of hypersonic applications to achieve much better performance than the conventional wing configurations.

However, it's not quite easy for grid fin using in hypersonic flying which will be affected by the flow field, thermal field and structure field at the same time. The air flows opposite to the wings and provides lift force for the flight vehicle, while the wings stressed and deformed conversely affects the distribution of the flow field. Air friction changes the surface temperature of the wings, and the temperature conversely affects the physical properties of structure and fluid. During the flight, it may encounter any or all of the following conditions: 1) extremely hot surface temperature; 2) large temperature gradients; 3) transient heating. In response to these extreme conditions, the grid fin may experience any or all of the following conditions: 1) possibly large thermal stress superimposed on aerodynamic pressure; 2) changes in material properties such as strength and elastic modulus; 3) high temperature creep. In addition, it's really difficult to obtain reliable experimental structural response with a complex fluid-thermal superposition boundary condition. Hence, there are many significant challenges in predicting structural response in such an extreme environments, including: 1) the simultaneous response of fluctuating pressures, aerodynamic heating and structure deflection over long durations; 2) material nonlinearity; 3) spatial variation of material and structure properties; 4) uncertainty in loads, material properties, geometry, and boundary conditions; and 5) the computational cost and complexity of large, coupled models.

Traditionally, in order to tackle those complex issues occurring in design process, an aerodynamicist will predict the surface pressures and heating rates by assuming a rigid isothermal body. These aerodynamic heating rates are used by a structural heat transfer analyst to predict the structure temperature distribution. Finally, a structural analyst uses the temperature distribution and aerodynamic pressure to predict the structural deformations and stresses. Such traditional independent approaches require several interactions between the different analysis methods and analysts. The approach is relatively inefficient and untrustworthy. Meanwhile, early theoretical calculations cannot fully reflect the coupling between the three physical fields of grid fin[8]. Even though a system of partial differential equations describing such problem is obtained, if it is not simplified, it's also difficult to get solved manually. In fact, in the early 1900s, Lamb et al. proposed the problem that such structure had an impact on other media[9]. After that, Whitehead[10] proposed a classic semi-empirical analysis method, *actuator disk*, for the numerical analysis of the flow field in 1959.

Whereas, because of other restrictions, not until the late 1960s when the numerical methods of finite element and boundary element came into being did the detailed analysis appear to solve the problem. In *Applied Mechanics Review* published by the American Society of Mechanical Engineers, there was no term of fluid-structure interaction from 1970 to 1980, and related terms were only aeroelasticity, tremor, etc. Not until 1981~1983 did the term fluid-structure interaction (FSI) began to come into being. With the establishment of the entry FSI, in these three years, the number of abstracts under this entry was up to 49, 73 and 50, which also shows certain development of fluid-structure interaction in the 1980s. In 1991, Bendiksen[11] was the first person to propose that fluid and structure domains could be solved through a unified equation, i.e. two-way media interaction. It meant that while the structure was solved, the force to the structure generated by the fluid should be explicitly solved. This forced decoupling method shows that people then began to use some effective ways to solve the problem of fluid-structure interaction. In 1992, Takashi[12] used Arbitrary Lagrange-Euler (ALE) for the description to solve the uniform hybrid equation and applied semi-implicit and semi-explicit method to the fluid and finally solve the N-S equation. In 2001, Choi[13] separated variables to solve the hybrid equation of fluid-structure interaction proposed by predecessors, who introduced the symmetrical pressure equation and applied the four-step method and ALE for the solution. From 2001 to 2004, Hubner[14-16] adopted the space finite element with discontinuous stabilized time to discretize the model equation, establish a single system of equations and solve the problem of flow around of two-dimensional viscous fluid. In 2005, Namkoong[17] proposed a method to directly solve the hybrid equation and address the problem of two-dimensional channel flow of two-dimensional vertical plate division. At the same time, in order to solve the problem of buckling and large deformation of the three-dimensional structure, Zhang and Hisada[18] jointly developed a program of FSI that provided a method to follow to solve fluid-structure interaction, who at the same time applied ALE to solve the fluid-structure interaction problem of two-dimensional heart beat and three-dimensional large deformation. Then, with the requirement of developing advanced hypersonic flight vehicle, the thermal influence was added in the fluid-structure coupling problem in order to synthesis the three fields interaction to support the structure design and the thermal protection system design for the hypersonic flight vehicle. In 2010, Culler[19] carried out the fluid-thermal-structure simulation on the hypersonic flight vehicle and validate the aerodynamic force and heating results with some wind tunnel test data. It shows goodness fit with the experiments and represent the future trends of flight vehicle design methodology in using fluid-thermal-structure integration method. Obviously, this method also suggests a new way of thinking about the grid fin designing and its application in hypersonic flight vehicle. In this paper, we presents a numerical approach to study the fluid-thermal-structure coupling problems of the grid fin. The influence factors of the attack angle on different field effect will be numerically discussed, and the structure response with two different material will also be revealed. The objective of this work is to provide investigators and designers of the grid fin with a relatively systematic reference.

## 2 NUMERICAL MODEL

### 2.1 Geometric model

In order to facilitate the verification of the reliability of the simulation method, this paper

established the geometric model of grid fin in accordance with reference literature[1]. The geometrical configuration and dimensions are shown in Figure 1. The grid fin is at the tail of the missile, which can work within a time of 200s, at a height of 20km and a flight speed of 6Ma.

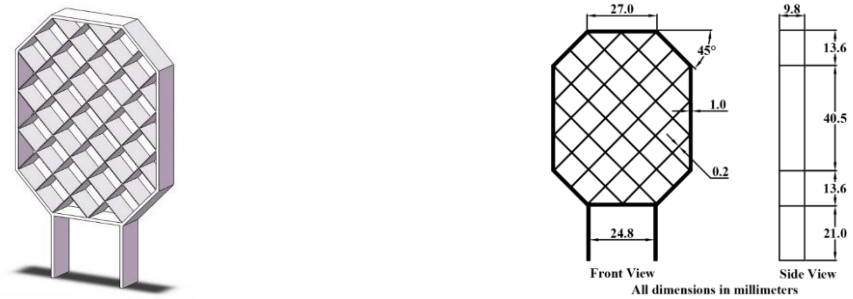


**Figure 1**: Geometric model and dimensions of grid fin

## 2.2 Flow field model

Figure 2 and 3 shows the mesh of flow field in ICEM. The minimum distance between the far field and the grid fin is 20 times of the chord length to ensure that the border will not interfere with the flow field around the grid fin. To facilitate the application of hexahedral mesh, the flow field is divided into multiblocks. On the contour of the fin, there are 118,883 nodes distributed, and after swept along the flow direction, a total of 13,465,840 units are generated. The grids on the boundary layer are densified.

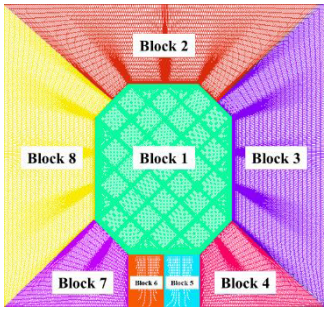


**Figure 2**: Local meshes distributed on flow direction

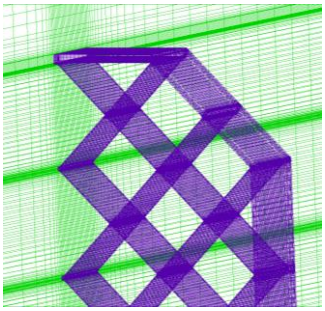

**Figure 3**: Local meshes distributed on grid fin surface

After the geometric model and mesh division are completed, the coupled areas need to be marked so that the corresponding coupling surface can be selected for the coupling calculation. The independent set is respectively named for inlet, outlet, far-field boundary of the flow field and the contour of grid fin. Reynolds-Averaged approach and Spalart-Allmaras turbulence model are employed to solve the problem of flowing fluid, and the second order upwind scheme is used to achieve the simulation.

## 2.3 Model validation

This paper makes reference to the simulation results of the grid fin in literature[1] and

makes comparison between the angle of attack and normal force coefficient curve to verify the correctness of the established geometry and grid of the flow field. The numerical model of grid fin is validated with the flow field parameters: 1) free incoming flow Mach number Ma=1.8, 2.5 and 3.5; 2) incoming flow temperature T=293.15K; 3) Reynolds number Re=$2.3\times10^6$, $3.0\times10^6$ and $4.7\times10^6$; 4) angle of attack α=0~15°and interval of 5°; 5) angle of sweepback δ=0, -15°. Through the numerical simulation at multiple angles of attack of grid fin, the relationship of change between the normal force coefficient and angle of attack is obtained, as shown in Figure 4 and 5. The grid fin's normal force coefficient increases gradually with the growth of the angle of attack. It can be seen from the comparison between the measured data and model values that at the same angle of attack the normal force coefficient of the grid fin is very close and the minimum error is less than 18% (δ=0°) and 22% (δ=-15°), therefore, the parameter settings and grid distribution of the flow field model are reasonable.

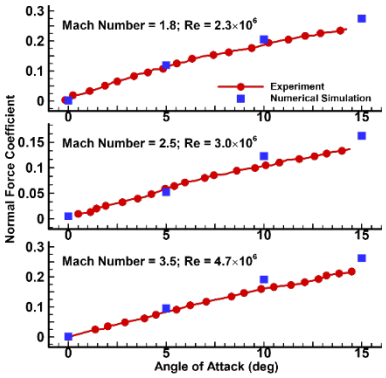


**Figure 4**: Normal force coefficient versus angle of attack, δ=0°

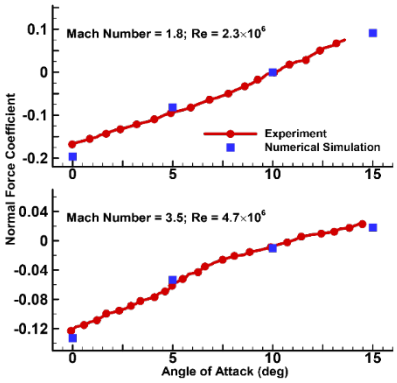


**Figure 5**: Normal force coefficient versus angle of attack, δ=-15°

## 3 NUMERICAL CALCULATION AND ANALYSIS

### 3.1 Coupling calculation strategy

For the coupling calculation of heat transfer between the flow field and the structure field, data exchange occurs on the wall contacting the flow field, called the coupling interface. Data repeatedly exchange on the coupling interface to satisfy the boundary conditions of the next calculation of the flow field and the structure field. The flow field requires new temperature boundary conditions provided by the coupling interface, while the structure field needs new heat flow boundary conditions. The coupling scheme in this paper is as follows:

(1) At the time t=0s, a steady-state solution of the flow field is first calculated under the wall boundary conditions at a constant temperature, and then the heat flow value on the coupling interface is obtained (heat flow transferred from the flow field to the wall), represented by $q_f$ ($f$ represents the flow field).

(2) Without wall radiation effect considered, according to energy conservation, the heat flow transferred from the wall into the structure field is equal to that from the flow field to the wall. So the heat flow boundary condition ($s$ represents the structure field) to calculate the

heat transfer of the structure field can be as follows:

$$k_s\left(\frac{\partial T_x}{\partial x}n_x+\frac{\partial T_y}{\partial y}n_y+\frac{\partial T_x}{\partial z}n_z\right)=q_f \tag{1}$$

(3) The above formula is taken as the boundary condition of the structure field for solving the heat transfer equation, and after a time of $\Delta t$ (the coupling time of this model is 1s), the temperature $T_s$ of the re-distributed field structure can be obtained (the structure field is in the uniform temperature state initially).

(4) After the calculation of a time step $\Delta t$ (FEM) of the structure field, the temperature boundary condition $T_s$ of the next calculated of the flow field can be obtained, i.e. the new wall temperature.

(5) At the temperature boundary $T_s$ the transient flow field calculation is carried out. After the time $\Delta t$, the new wall heat flow value $q_f$ can be obtained. Then this variable is extracted from the flow field and loaded into the structure field as a boundary condition, and the next calculation is carried out.

(6) The cycle is repeated until the end of the calculation.

### 3.2 Fluid thermal coupled

Actually, the validation model is used in the wind tunnel test and too small to be applied for the authentic flight vehicle. Hence, with considering the practical application, a major difference is that the calculation model is 10 times larger than the validation model. Meanwhile, the model is calculated in Ma=6 of free incoming flow at the angles of attack from 0 to 15°. By the calculation, the pressure and heat flux is obtained. Figure 6 shows the nephogram results of surface pressure after 200s flights in different angles of attack. It can be found that, in Figure 6(a), the high pressure area on the grid fin surface are mainly distributed in the region of the leading edge stagnation point, where the maximum pressure is 0.27 MPa. However, with the increasing of angle of attack, the high pressure area are no longer staying in the leading edge region due to the complex shock and expansion wave interaction between the inner lattice wings. Moreover, in Figure 6(c), the result shows that the area occurs in the leeside of gird fin which is totally different from the patchy distributions of angle 5° and 15°.

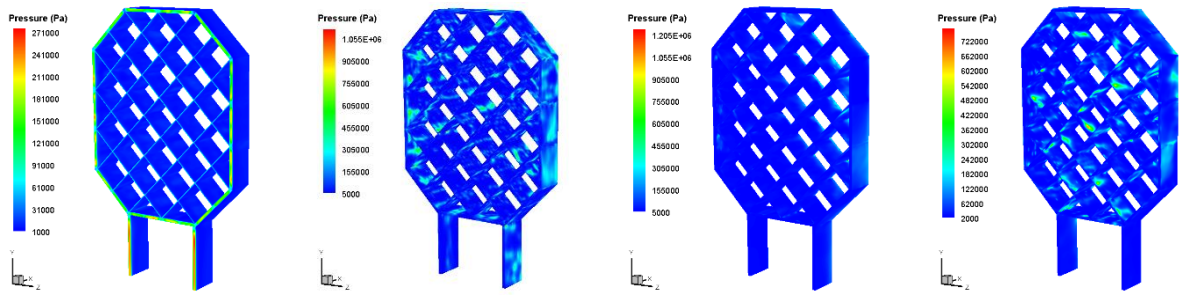


(a) α=0° (b) α=5° (c) α=10° (d) α=15°

**Figure 6**: Surface pressure nephogram in different angles of attack

Figure 7 shows the nephogram results of heat flux in different angles of attack. The

distributing characteristics are displayed similar to Figure 6 and most area is graded in megawatt per square meter. As the Figure 6 and 7 show, it cannot be simply asserted that the leading edge of the grid fin will be the most severe region of aerodynamic heating as well as the design focus of thermal protection of the structure which just only happened in 0° attack angle. Due to the complex flow separation, the thermal protection design should synthesize each kind of situation. In addition, it should also be noted that the high pressure and heat flux environment will further promote heat exchange between the flow field and the structure field, therefore, to get the further structure response will be the focus of study on the use under hypersonic conditions.

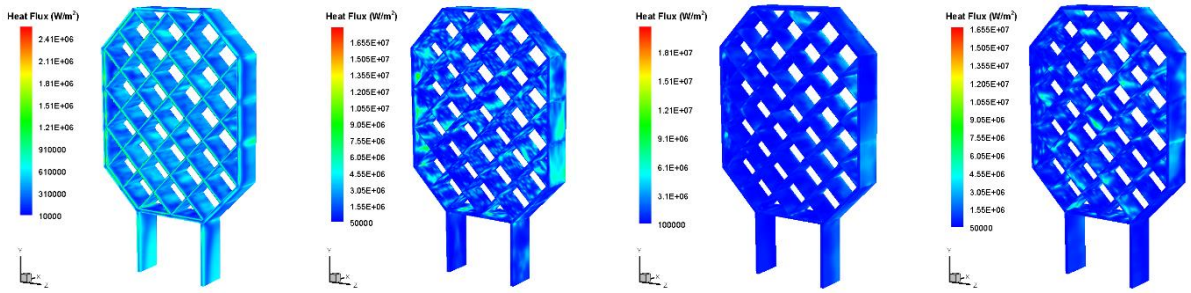


(a) α=0° (b) α=5° (c) α=10° (d) α=15°

**Figure 7**: Heat flux nephogram in different angles of attack

### 3.3 Structure response

During a long time flying with the combination of extreme pressure and heat, general metal alloy is difficult to bear, so that, some high temperature materials are taken into account. Firstly, the niobium alloy which could provide an excellent high specific strength from 1093°C to 1427°C is introduced in the coupled calculation with some considerations of its good mechanical property and a broad application scope of temperature. Some properties are shown in the following table:

**Table 1**: Material properties of niobium alloy

| Temperature K | Density kg/m$^3$ | Thermal conductivity W/(m·K) | Elasticity modulus GPa | Poisson ratio | Linear expansion coefficient $\times10^{-6}$(K$^{-1}$) | Specific heat J/(kg·K) |
|---|---|---|---|---|---|---|
| 1150 | 8800 | 37.4 | 103 | 0.3 | 8 | 273 |
| 1580 | 8800 | 42.4 | 112 | 0.3 | 10 | 327.6 |

About the boundary condition, the displacement restrictions through x, y and z orientation are applied to the bottom holder of grid fin, the initial temperature of the structure is set as 295.15K. The wall boundary of grid fin is treat as the coupling area for exchanging and transferring variable data, the data of coupling is the heat flux variable which will be extracted through the fluid field calculation, at the same time, the temperature variable also could be picked up after the structure field calculation for the next coupling step.

Figure 8 shows the temperature distribution of the grid fin in using niobium alloy after 200s simulation. As the figure shows, in 0° angle of attack, the highest temperature is up to

1127K and rapidly declines along the longitudinal direction; in 5°, the temperature of bottom holder sharply climbed to more than 1500K, some area is even as high as 2500K; in 10°, the trailing edge occurs extreme high temperature as the heat flux distribution of Figure 6(c); in 15°, the leading edge becomes the most serious area again as Figure8(a), but the temperature distribution of bottom holder is mostly the same as Figure 6(c). More generally, the temperature distribution is inhomogeneous caused by the differential of heat flux and most region has reached more than 500K, some local area has risen by over 1500K which is the maximum working temperature of niobium alloy.

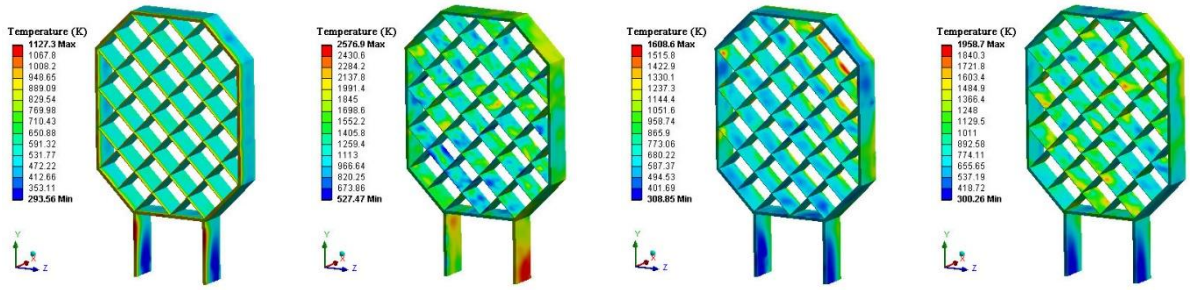


(a) α=0° (b) α=5° (c) α=10° (d) α=15°

**Figure 8**: Temperature nephogram of niobium alloy in different angles of attack

The drastic temperature gradients will further effect the strength and stiffness of the structure. As the Figure 9 shows, the average stress level increases with the increasing of attack angle. It should be also noted that, with the existence of the sharp corner, significant stress concentration appears especially for the bottom holder which is one of the weak parts of the main structure and need to be further optimized.

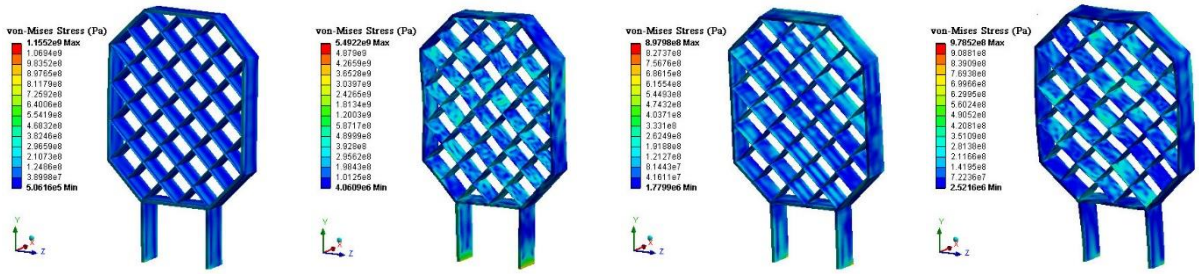


(a) α=0° (b) α=5° (c) α=10° (d) α=15°

**Figure 9**: Von-Mises stress nephogram of niobium alloy in different angles of attack

As the displacement nephogram shows in Figure 10 which is got from the calculation results, an interesting phenomenon is found that the displacement is not simply enlarged with the increasing of attack angle, in 5°, an obvious extrusion takes place at the left and right edge of the outer frame and in 15°, by contrast, the expansion appears. Furthermore, the maximum displacement reaches 14.5mm that severely impact the aerodynamic configuration for supplying lifting force. Actually, in this model, some more detail properties (e.g. failure strength, fracture strength, etc.) are not added in the calculation when the working temperature exceed to 1500K in order to reduce the intolerable time cost. The structure will

be cracked in such an extreme environment under the alternate loading over the long period of time.

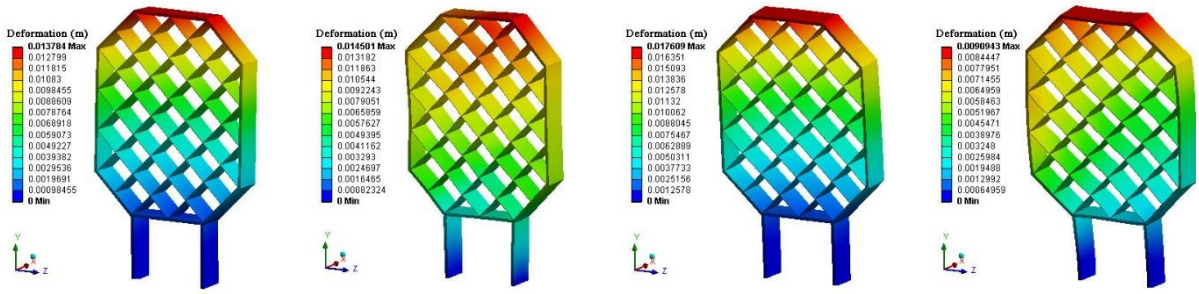


(a) α=0° (b) α=5° (c) α=10° (d) α=15°

**Figure 10**: Displacement nephogram of niobium alloy in different angles of attack

It is with these thoughts in mind that the niobium alloy will no longer take into account due to the excess of its working temperature and large displacement caused by the high pressure and temperature environment, so some other materials should be sought to satisfy this environment. Based on the preliminary calculation results before, the C/SiC composites is used to replace the niobium alloy. It can almost meet all the need of hypersonic application: long life (under 1950K), finite life (under 2300K), and transient life (under 3100K). Here are some basic material properties listed in the following table:

**Table 2**: Material properties of C/SiC composites

| Temperature K | Density kg/m$^3$ | Thermal conductivity W/(m·K) | Elasticity modulus GPa | Poisson ratio | Linear expansion coefficient $\times 10^{-6}$(K$^{-1}$) | Specific heat J/(kg·K) |
|---|---|---|---|---|---|---|
| 295.15 | 2000 | 8 | 124 | 0.06 | 0.38 | 800 |
| 300 | 2000 | 8 | 112 | 0.06 | 3.09 | 900 |
| 600 | 2000 | 8 | 102 | 0.06 | 3.72 | 1200 |
| 900 | 2000 | 8 | 83 | 0.06 | 3.41 | 1500 |
| 1100 | 2000 | 8 | 91 | 0.06 | 4.49 | 1700 |
| 1300 | 2000 | 8 | 68 | 0.06 | 3.68 | 1700 |
| 1390 | 2000 | 8 | 33 | 0.06 | 4.01 | 1800 |

Through the comparison of temperature distribution between Figure 8 and 11, it was found that the maximum temperature of C/SiC composites is about 259K, 214K, 180K and 190K higher than the niobium alloy. It's mainly because of their closely thermal conductivity and a lower heat capacity compared with niobium alloy.

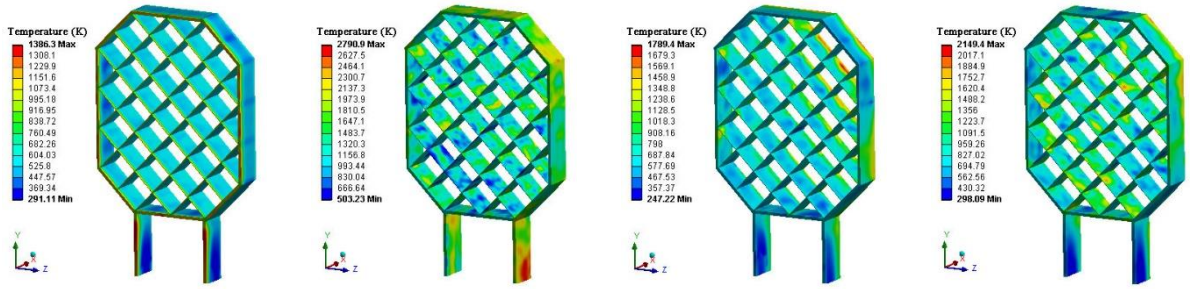


(a) α=0° (b) α=5° (c) α=10° (d) α=15°

**Figure 11**: Temperature nephogram of C/SiC composites in different angles of attack

Figure 12 shows the final stress distribution of the C/SiC composites structure. Although the elasticity modulus of C/SiC composites has fallen by almost 70% in comparison to the property under ambient temperature, however, the slow growth of expansion coefficient with temperature rise will prevent the increase of thermal stress and displacement, hence, the stress level in Figure 12 is about half lower than the niobium alloy.

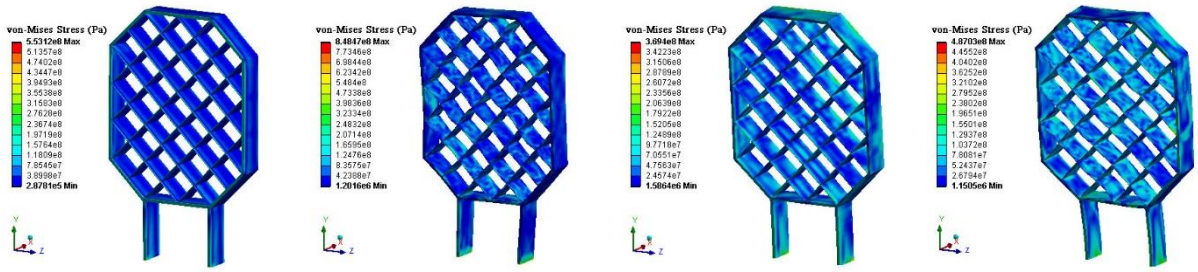


(a) α=0° (b) α=5° (c) α=10° (d) α=15°

**Figure 12**: Von-Mises stress nephogram of C/SiC composites in different angles of attack

The displacement in Figure 13 exhibits that the deformation of C/SiC composites structure is 40%, 57%, 35% and 27% lower than niobium alloy. In addition, it is noticed that, in 5° and 15° attack angle, the bottom holder happens some lateral displacement influenced by the mixture load, the supporter should be enhanced to deter the lateral load.

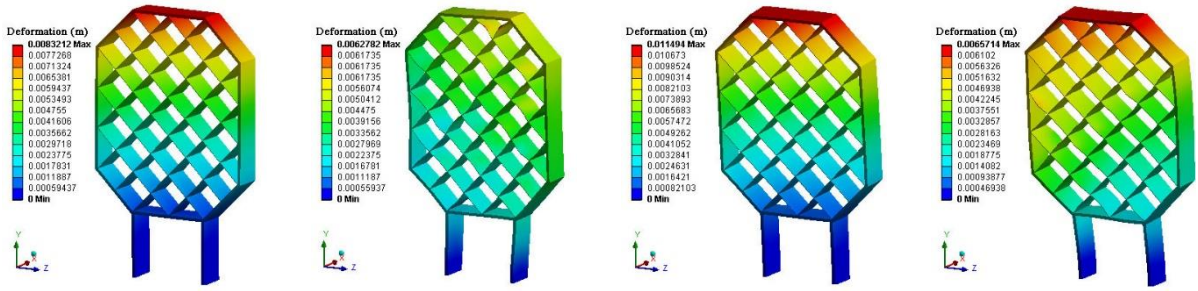


(a) α=0° (b) α=5° (c) α=10° (d) α=15°

**Figure 13**: Displacement nephogram of C/SiC composites in different angles of attack

## 4 CONCLUSIONS

This paper has analyzed the characteristics of fluid-thermal-structure interaction of grid fin under hypersonic conditions and makes comparison with former researches to verify the reliability of the calculation scheme. Following conclusions can be reached:

(1) The value of normal force coeffecient is very close to the calculation results of the literature, and the reliability and effectiveness of the model is verified by simulations.

(2) With the increasing of attack angle, the most serious region of aerodynamic pressure and heat flux no longer concentrate on the stagnation point of leading edge, the temperature, stress and displacement distribution changed followed by. The maximum value of temperature, stress and deformation occurs at the 5° attack angle.

(3) The deformation and stress level of C/SiC composites are better than the niobium alloy, however, in this situation, the composites not fit for long time using under a fix attack angle.

(4) The current configuration exhibits good resistance to bending, meanwhile, some lateral area should be paid attention especially for the root of bottom holder.

The results provide a reference for the design of the heat-resistant structure of grid fin.

## REFERENCES

[1] Washington, W.D. and Miller, M.S. *Grid fins - a new concept for missile stability and control*. Reno: 31st Aerospace Sciences Meeting & Exhibit, (1993).

[2] Belotserkovskiy, S.M., Odnovol, L.A., Safin, Y.Z. and et al. *Wings with internal framework*. Mashinostroeniye, Vol. I, (1987).

[3] Sun, Y. and Khalid, M. *A cfd investigation of grid fin missiles*. Cleveland: 34th AIAA/ASME/SAE/ASEE Joint Propulsion Conference and Exhibit, (1998).

[4] Theerthamalai, P. Aerodynamic characterization of grid fins at subsonic speeds. *J. Aircr.* (2007) **44**:694-697.

[5] Simpson, G.M. and Sadler, A.J. *Lattice controls: A comparison with conventional, planar fins*. Sorrento: the RTO AVT Symposium, (1998).

[6] Reynier, P., Reisch, U., Longo, J. and et al. *Numerical study of hypersonic missiles with lattice wings using an actuator disk*. Missouri: 20th AIAA Applied Aerodynamics Conference, (2002).

[7] Schülein, E. and Guyot, D. *Novel high-performance grid fins for missile control at high speeds: Preliminary numerical and experimental investigations*. Neuilly-sur-Seine: RTO-MP-AVT, (2006).

[8] Wang, D. and Yu, Y. *Numerical study on drag reduction for swept-back, swept-front , delta grid fin with blunt and sharp leading edges*. National Harbor: AIAA Modeling and Simulation Technologies Conference, (2014).

[9] Mathews, I.C. Numerical techniques for three‐dimensional steady‐state fluid‐structure interaction. *J. Acoust. Soc. Am.* (1986) **79**:1317-1325.

[10] Whitehead, D.S. Vibration of cascade blades treated by actuator disc methods. *P. I. Mech. Eng.* (1959) **173**:555-574.

[11] Bendiksen, O. *A new approach to computational aeroelasticity*. Baltimore: 32nd Structures, Structural Dynamics, and Materials Conference, (1991).

[12] Takashi, N. and Hughes, T.J.R. An arbitrary lagrangian-eulerian finite element method for interaction of fluid and a rigid body. *Comp. Meth. Appl. Mech. Eng.* (1992) **95**:115-138.
[13] Choi, H.G. and Joseph, D.D. Fluidization by lift of 300 circular particles in plane poiseuille flow by direct numerical simulation. *J. Fluid Mech.* (2001) **438**:101-128.
[14] Hubner, B., Walhorn, E. and Dinkier, D. *Strongly coupled analysis of fluid-structure interaction using space-time finite elements*. Cracow: 2nd European Conference on Computational Mechanics, (2001).
[15] Hubner, B., Walhorn, E. and Dinkler, D. *Simultaneous solution to the interaction of wind flow and lightweight membrane structures*. Warsaw: Proceedings of International Conference on Lightweight Structures in Civil Engineering, (2002).
[16] Hübner, B., Walhorn, E. and Dinkler, D. A monolithic approach to fluid–structure interaction using space–time finite elements. *Comp. Meth. Appl. Mech. Eng.* (2004) **193**:2087-2104.
[17] Namkoong, K., Choi, H.G. and Yoo, J.Y. Computation of dynamic fluid–structure interaction in two-dimensional laminar flows using combined formulation. *J. Fluid Struct.* (2005) **20**:51-69.
[18] Zhang, Q. and Hisada, T. Studies of the strong coupling and weak coupling methods in fsi analysis. *Int. J. Numer. Meth. Eng.* (2004) **60**:2013-2029.
[19] Culler, A.J. *Coupled fluid-thermal-structural modeling and analysis of hypersonic flight vehicle structures*. PhD: The Ohio State University, (2010)